



Implementation of the “Harmonic Variables” Concept in the Vibration Analysis of a Coupled Rotor/Fuselage System*

S. M. BARKAI AND O. RAND

Faculty of Aerospace Engineering

Technion—Israel Institute of Technology, Haifa 32000, Israel

(Received November 1994; accepted January 1995)

Abstract—The paper presents a new numerical technique for deriving and solving the nonlinear periodic equations of motion of a coupled rotor/fuselage system. The method is based on the combination of the concept of working with “Harmonic Variables” with general purpose nonlinear solvers. The resulting technique substantially reduces the required analytical effort while preserving high accuracy solution and symbolic harmonic resolution. For demonstration purposes, the present nonlinear modelling consists of elastic blades and fuselage, and contains nonlinear elastic and dynamic contributions. The method is demonstrated by a study of the influence of possible fuselage responsiveness on the vibratory hub motion and hub loads.

1. INTRODUCTION

The prediction of the vibratory response of coupled rotor-fuselage systems poses many modelling and computation challenges and has attracted considerable research efforts during the last decade [1]. The fact that these systems undergo vibration in all their operation modes creates a need for adequate prediction of their vibratory characteristics even in the early design stages. Moreover, many of the advanced active mechanisms for vibration reduction (and recently also for improving the rotor acoustic characteristics) in helicopters are based on introducing high harmonic pitch commands to the blade root [2–6]. Among these vibration suppression methods it is important to mention the well known Higher Harmonic Control (HHC) technique [2–5], which is implemented through a conventional swashplate and provides identical excitation for all blades, and the Individual Blade Control (IBC) technique [6] which produces different high harmonic pitch commands for each blade. Clearly, the key to meaningful estimation of the efficiency of such methods is a high quality prediction of the vibratory characteristics of the involved rotor-airframe systems. Such prediction should be able to handle nonlinear effects that might originate from the elastic, the dynamic and the aerodynamic modelling, and should preserve high harmonic resolution (see also [7,8]).

There are numerous contributors to the complexity of the analysis of rotary wing-airframe systems and many sources of computation difficulties. From an aerodynamic point of view, it may be stated that the unsteady aerodynamic environment which is created by the rotary wing presence, introduces various complications to the unsteady loads predictions (unsteady motion of the blades, interlocking wakes, wake-airframe interaction, etc.) and usually force a number of

*Presented at the 20th European Rotorcraft Forum, Amsterdam, The Netherlands, October 4–7, 1994. The authors would like to acknowledge the figures drawn by the late Ruth Public.

major simplifying assumptions. From a dynamics point of view, the coupling between the rotor and the fuselage results in a nonlinear formulation in which the hub vibratory motion and loads have to be balanced. There are also significant elastic motions of the blades and the fuselage which contribute nonlinearities and an enormous number of additional degrees of freedom.

Clearly, the mathematical formulation of the vibratory response of coupled rotor/fuselage systems leads to the construction of periodic equations. The direct way to formulate these equations is based on spectral methodologies and is generally known as “Generalized Harmonic Balance.” References [9–12] are representative studies where this approach has been applied in rotorcraft systems. Although the harmonic balance method is a simple approach, its implementation in highly nonlinear equations where high resolution is required (i.e., high number of harmonics should be included), still poses some analytical and numerical difficulties. The main difficulties emerge from the fact that the vibratory phenomena are extremely small fluctuations of the mean and the first harmonics components of the loads. Therefore, in order to be able to accurately predict these small components, a large number of harmonics should be included, and the evaluation of the resultant vibratory components should be executed in a suitable manner which will preserve the influence of the high harmonics, and will prevent errors induced by the relatively large low harmonics. The present paper offers a new numerical technique that enables simple and symbolically exact evaluation of periodic expressions. These characteristics of the proposed method, supported with additional numerical techniques that will be described in this paper, provide a new tool that overcomes the above difficulties.

The general aspects of the method will be described and discussed first, followed by a few numerical results of a study of the influence of a broad range of possible elastic fuselage responsiveness on the vibratory hub motion and hub loads.

2. THE NUMERICAL PROCEDURE

2.1. General Algorithms for Nonlinear Systems

The present method of solution is based on the combination of the “Harmonic Variables” concept with generic algorithms for solving nonlinear systems. To appreciate the advantages offered by this concept, it is first necessary to put in perspective all methods for nonlinear periodic response. The reader should carefully distinguish between “methods for periodic response” which are in the focus of the present paper and are designed to determine the steady state periodic response, and “time integration methods” which are capable of simulating the transient response (and may also reach the periodic response after the integration is carried out for a number of periods, and the transient response is diminished).

Generally, numerical solution procedures for nonlinear periodic equations are based on two major steps:

- (a) The conversion of the nonlinear periodic differential equations to the form of nonlinear algebraic equations using “stationary unknowns.”
- (b) The solution of the resulting algebraic system of equations.

There are several ways to execute the first step (step (a)). For example, while using the Fourier series expansion, the stationary unknowns are the harmonic coefficients. Similarly, there are other versions of expanding the unknowns in terms of *a priori* defined shape functions. Using the “finite-element in time” technique, the stationary unknowns are the values and the derivatives of the original unknowns at some prescribed azimuthal locations. Once the system of nonlinear periodic equations is formulated as a system of nonlinear algebraic equations, it may be solved by well established numerical tools (step (b)). Thus, the most critical stage in any formulation is the conversion of the system to the form of a system of algebraic equations.

The purpose of the method proposed in this paper is to present a new way to efficiently and accurately execute the first step mentioned above, i.e., to convert the system into a system of

algebraic equations while preserving all nonlinearities and maintain symbolic harmonic resolution. However, before describing the method, and in order to clarify the picture, the working mode of a generic nonlinear solver will be described first. For that purpose, the following generic nonlinear algebraic system is considered:

$$r_i(x_1, x_2, \dots, x_n) = 0, \quad i = 1, n, \quad (1)$$

where $\{x_i\} = \langle x_1, x_2, \dots, x_n \rangle^\top$ is the vector of independent unknowns (“unknowns vector”) and $\{r_i\} = \langle r_1, r_2, \dots, r_n \rangle^\top$ contains the equation residuals (“residual vector”). A general purpose nonlinear solver is designed to determine the unknowns vector $\{x_i^s\}$ that will satisfy equation (1), and is usually based on two main components as shown by Figure 1. The first component is “The Algorithm” which includes the logic of the nonlinear solution (such as the Newton-Raphson method, quasi-linear iterations, etc.). Starting from an “initial guess vector,” $\{x_i^0\}$, this component reaches the desired solution by successive substitutions of “trial vectors,” $\{x_i^t\}$, in the second component that may be titled “The Equations.” This component evaluates the equation residuals $\{r_i\}$ for each trial vector. Depending on the solution algorithm, the trial vectors are selected in a way that the “solution vector” $\{x_i^s\}$ may be deduced.

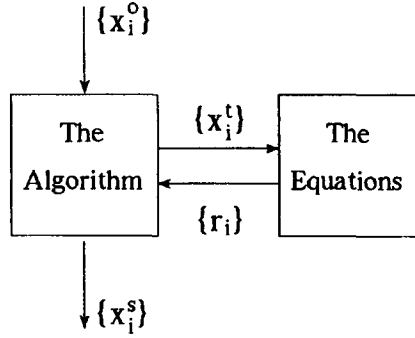


Figure 1. Scheme of nonlinear solver operation mode.

To describe the proposed way to execute the above step (a), (i.e., “The Equations” part in Figure 1), the concept of working with Harmonic Variables is described next.

2.2. The Harmonic Variables Concept

In general, the “Harmonic Variables” concept is based on the definition of Harmonic Variables, mathematical operations with them and their usage in deriving the equations of motions. These aspects will be discussed in this section. More details are given in [13].

2.2.1. Definition

A Harmonic Variable is a real number the value of which varies periodically with a period of 2π . Harmonic Variable, F , may therefore be represented by an infinite array of its Fourier coefficients as:

$$F = F_0 + \sum_{p=1}^{\infty} [F_{cp} \cos(p\psi) + F_{sp} \sin(p\psi)]. \quad (2)$$

Truncating the above infinite sum enables one to define the Harmonic Variable, F , by a finite harmonic operator, H_q , using finite arrays of real numbers F_{cp} and F_{sp} of dimension q (i.e., $p = 1, \dots, q$) as:

$$F \cong H_q(F_0, F_{cp}, F_{sp}) \equiv F_0 + \sum_{p=1}^q [F_{cp} \cos(p\psi) + F_{sp} \sin(p\psi)]. \quad (3)$$

In principle, the periodicity parameter, ψ , may represent any variable. However, in the context of the present study, ψ represents a nondimensional time (i.e., $\psi = 2\pi t/T$ where t is the time and T is the period). In what follows, all Harmonic Variables and their coefficients will be denoted as shown in equation (3) (i.e., denoting the harmonics by the subscripts $()_0$, $()_{cp}$ and $()_{sp}$). Clearly, any constant real number, r , may be represented as the Harmonic Variable, R , where $R_0 = r$, $R_{cp} = R_{sp} = 0$ ($p = 1, \dots, q$). In addition, the basic trigonometric functions $\sin(\psi)$ and $\cos(\psi)$ may be described as the Harmonic Variables S and C , respectively, where $S_{s1} = C_{c1} = 1$ and $S_0 = C_0 = S_{c1} = C_{s1} = 0$, $S_{cp} = S_{sp} = C_{cp} = C_{sp} = 0$ ($p = 2, \dots, q$).

Practically, Harmonic Variable may be viewed as an array of real numbers and this is the way it is stored in the numerical codes. For example, the Harmonic Variable, E , is stored as an array of the real numbers $E_0, E_{c1}, \dots, E_{cq}, E_{s1}, \dots, E_{sq}$.

2.2.2. Mathematical operations

Based on the above definition, it is possible to define arithmetic and general mathematical operations between Harmonic Variables. Additions and subtractions are trivial and are essentially based on adding or subtracting the corresponding harmonics. Multiplying two Harmonic Variables is based on the appropriate trigonometric identities and may be put in the following form for the case of $E = F \bullet G$:

$$\begin{Bmatrix} E_0 \\ E_{c1} \\ \vdots \\ E_{cq} \\ E_{s1} \\ \vdots \\ E_{sq} \end{Bmatrix} = [\bar{G}] \begin{Bmatrix} F_0 \\ F_{c1} \\ \vdots \\ F_{cq} \\ F_{s1} \\ \vdots \\ F_{sq} \end{Bmatrix}, \quad (4)$$

where $[\bar{G}]$ is a matrix which is a function of the coefficients of the harmonic variable G only, namely: G_0, G_{cp}, G_{sp} ($p = 1, \dots, q$). This matrix is generated symbolically for any given number of harmonics. For example, in the case of $q = 3$, $[\bar{G}]$ is given by:

$$[\bar{G}] = \frac{1}{2} \begin{bmatrix} 2g_0 & g_{c1} & g_{c2} & g_{c3} & g_{s1} & g_{s2} & g_{s3} \\ 2g_{c1} & 2g_0 + g_{c2} & g_{c1} + g_{c3} & g_{c2} & g_{s2} & g_{s1} + g_{s3} & g_{s2} \\ 2g_{c2} & g_{c1} + g_{c3} & 2g_0 & g_{c1} & g_{s3} - g_{s1} & 0 & g_{s1} \\ 2g_{c3} & g_{c2} & g_{c1} & 2g_0 & -g_{s2} & -g_{s1} & 0 \\ 2g_{s1} & g_{s2} & g_{s3} - g_{s1} & -g_{s2} & 2g_0 - g_{c2} & g_{c1} - g_{c3} & g_{c2} \\ 2g_{s2} & g_{s1} + g_{s3} & 0 & -g_{s1} & g_{c1} - g_{c3} & 2g_0 & g_{c1} \\ 2g_{s3} & g_{s2} & g_{s1} & 0 & g_{c2} & g_{c1} & 2g_0 \end{bmatrix}. \quad (5)$$

Division of Harmonic Variables is essentially the inverse operation of the above multiplication operation. More details may be found in [13].

It should be noted that there is an interesting analogy between the number of coefficients needed to execute a mathematical operation between two Harmonic Variables and the number of digits needed to execute a mathematical operation between two real numbers. This is due to the fact that, similar to real numbers, adding and subtracting of Harmonic Variables do not change the required number of coefficients. However, multiplying two Harmonic Variables represented by q_1 and q_2 harmonics, respectively, results in a Harmonic Variable having $q_1 + q_2$ coefficients, and generally, division of two Harmonic Variables results in an infinite number of additional harmonics.

Similar to real numbers, analytic functions of Harmonic Variables (i.e., $F = f(G)$ or $F = f(G, E)$, etc.) may be easily executed based on the above basic arithmetic operations.

Differentiation of Harmonic Variables with respect to the periodicity parameter, ψ , results in Harmonic Variables as well:

$$\frac{\partial^n F}{\partial \psi^n} = (-1)^{(n+1)/2} H_q(0, -p^n F_{sp}, p^n F_{cp}), \quad n = 1, 3, 5, \dots, \quad (6a)$$

$$\frac{\partial^n F}{\partial \psi^n} = (-1)^{n/2} H_q(0, p^n F_{cp}, p^n F_{sp}), \quad n = 2, 4, 6, \dots \quad (6b)$$

It should be emphasized that all numerical schemes for differentiation and integration with respect to any variable (other than ψ) that have been developed for real numbers may be directly applied to Harmonic Variables as well, and may be executed using the above mathematical operations. The above operations also enable the construction of all other trigonometric functions by using the definitions of the sine and cosine functions (see Section 2.2.1).

2.3. Computerized Implementation

The implementation of harmonic variables in numerical codes is carried out using a “super compiler” which has been developed along the above guidelines. This is a computer code that converts codes that were written using Harmonic Variables to standard computer codes. As mentioned earlier, the Harmonic Variables are stored as arrays of real numbers and as far as the user is concerned, all mathematical operations with Harmonic Variables, (additions, multiplications, analytical functions, etc.) are written in the standard form as if they were real numbers.

A simple application of the method is presented in Figure 2. In this example, a short code is presented. The purpose of this code is to multiply two periodic functions: $1 + 2 \sin \psi + 3 \cos 2\psi$ and $4 + 5 \sin 3\psi + 6 \cos 4\psi$. First, each one of these two functions is declared as “Harmonic Variable” (of 17 coefficients: one for the constant value, 8 for the sine terms and 8 for the cosine terms), and denoted as HA and HB, respectively. Then, numerical values are assigned for all coefficients and HA and HB are printed out. As shown, the multiplication operation is subsequently executed as if these two periodic functions were real numbers by the ‘HC=HA*HB’ operation without any additional derivation or coding. The resulting Harmonic Variable, HC, is then printed out.

2.4. Application to the Equations of Motion

To derive the equations of motion using the present approach, all time-dependent quantities are first defined as Harmonic Variables while the “unknown vector” $\{x_i\}$ (see Section 2.1) contains the coefficients of all independent Harmonic Variables. Thus, for each “trial vector” $\{x_i^t\}$, the independent unknowns may be determined as Harmonic Variables. Explicit execution of the equations of motion in their homogeneous form yields the equations residuals in the form of Harmonic Variables as well. The harmonic coefficients of these residuals are then introduced to the “residual vector” $\{r_i\}$. Thus, since operations between Harmonic Variables are executed automatically (see for example the multiplication operation in Figure 2), the only requirement on the user part is the explicit coding of the nonlinear equations of motions, while no additional adaptation or time discretization is needed. Consequently, the required effort is reduced to the effort needed in a similar steady problem. In principle, the method is equivalent to the “harmonic balance” method that has lost its attraction due to the enormous analytical effort which was required for its employment while highly nonlinear terms are included. The proposed technique removes this difficulty. Moreover, increasing the number of harmonics does not cause any changes in the analytic derivation or in the computer code, and it is executed automatically by changing the Harmonic Variables dimension (q) in the mathematical operation routines.

It should be emphasized that this method is substantially different from other methods that use computerized symbolic manipulation tools. The symbolic operations are executed within the

```

C
C   Declaring HA,HB,HC as Harmonic Variables
C   of 8 harmonics(i.e. 17 coefficienth)
C   and double precision (*8).
C
C       HARMONIC(17)*8 HA,HB,HC
C
C   Setting HA to be:
C   1.+2.*Sin(Psai)+3.*Cos(2.*Psai)
C
C       HA=SET(0.D0)
C       HA=INPUTC(1.D0,0)
C       HA=INPUTS(2.D0,1)
C       HA=INPUTC(3.D0,2)
C
C   Printing HA
C
C       WRITE(10,*)'----- HA -----'
C       HA=PRINT(HA)
C
C   Setting HB to be:
C   4.+5.*Sin(3.*Psai)+6.*Cos(4.*Psai)
C
C       HB=SET(0.D0)
C       HB=INPUTC(4.D0,0)
C       HB=INPUTS(5.D0,3)
C       HB=INPUTC(6.D0,4)
C
C   Printing HB
C
C       WRITE(10,*)'----- HB -----'
C       HB=PRINT(HB)
C
C   Setting HC=HA*HB
C
C       HC=HA*HB
C
C   Printing HC
C
C       WRITE(10,*)'----- HC -----'
C       HC=PRINT(HC)
C
C   STOP
C   END

```

(a) The code (includes the input and a multiplication operation).

```

----- HA -----
0      1.0000      0.00000E+00
1      0.00000E+00      2.0000
2      3.0000      0.00000E+00
3      0.00000E+00      0.00000E+00
4      0.00000E+00      0.00000E+00
5      0.00000E+00      0.00000E+00
6      0.00000E+00      0.00000E+00
7      0.00000E+00      0.00000E+00
8      0.00000E+00      0.00000E+00
----- HB -----
0      4.0000      0.00000E+00
1      0.00000E+00      0.00000E+00
2      0.00000E+00      0.00000E+00
3      0.00000E+00      5.0000
4      6.0000      0.00000E+00
5      0.00000E+00      0.00000E+00
6      0.00000E+00      0.00000E+00
7      0.00000E+00      0.00000E+00
8      0.00000E+00      0.00000E+00
----- HC -----
0      4.0000      0.00000E+00
1      0.00000E+00      15.500
2      26.000      0.00000E+00
3      0.00000E+00      -1.0000
4      1.0000      0.00000E+00
5      0.00000E+00      13.500
6      9.0000      0.00000E+00
7      0.00000E+00      0.00000E+00
8      0.00000E+00      0.00000E+00

```

(b) The output.

Figure 2. An application of "Harmonic Variables."

mathematical operations during the numerical execution of the code and are never written nor coded explicitly. Nonlinear expressions are evaluated gradually using the required mathematical operations as if all Harmonic Variables were real numbers. The fact that each mathematical operation preserves symbolic exactness provides this kind of exactness to the entire expression. Unlike the standard symbolic manipulation tools, the present method enables the introduction of decisions and conditioning elements to the code based on momentary values of the variables.

2.5. "Dynamic" Scaling

The nonlinear solvers mentioned above usually use convergence criteria which are based on the norm of the "unknowns vector." Therefore, if the numerical values of the unknowns differ by few orders of magnitude, only the relatively large components of the "unknowns vector" will influence the norm, which is bound to induce numerical errors in the evaluation of the relatively small components.

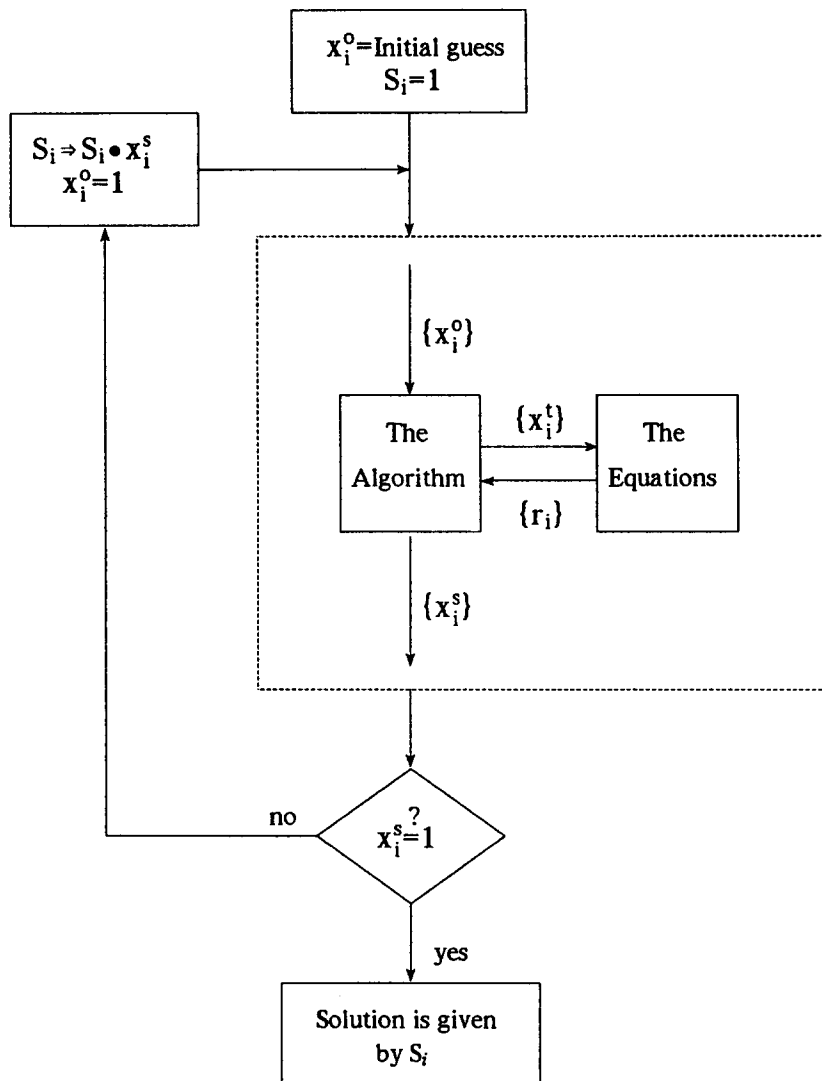


Figure 3. The application of "dynamic scaling."

Examination of the order of the numerical magnitude of the unknowns in a typical rotor/fuselage system shows vast variety. For example, the numerical values of the 4th harmonic components of the blades beamwise elastic motion may be considerably smaller than the constant (mean) one, but it plays a major role in the vibration analysis. Clearly, nondimensionalization based on

physical arguments does not solve this problem. Therefore, to maintain high resolution, a special “dynamic” scaling method has been developed—see Figure 3. In this method, the scaling factors are initially set to unit for all unknowns, i.e., $S_i = 1$ ($i = 1, N$). Then, the nonlinear solver is activated and the resulting “solution vector” $\{x_i^s\}$ is used to determine a new set of scaling factors which are equal to $S_i \cdot x_i^s$ ($i = 1, N$). When such iterations are repeated, the resulting solution vector is converged to a unit vector (i.e., $x_i^s = 1$, $i = 1, N$) and the solution is given by the last scaling factors vector. In this way, all unknowns are forced to equally contribute to the norm regardless of their numerical value.

3. THE ROTOR/FUSELAGE SYSTEM

A brief description of the rotor/airframe system modelling which has been used to demonstrate the proposed method of solution is described in this section. More details may be found in [14].

3.1. Degrees of Freedom

The modelling is based on five systems of coordinates which are connected by exact transformation matrices based on Euler finite angles. The systems are described in Figures 4 and 5. Each system and quantities in its directions are denoted by one of the indices G , F , H , B and D .

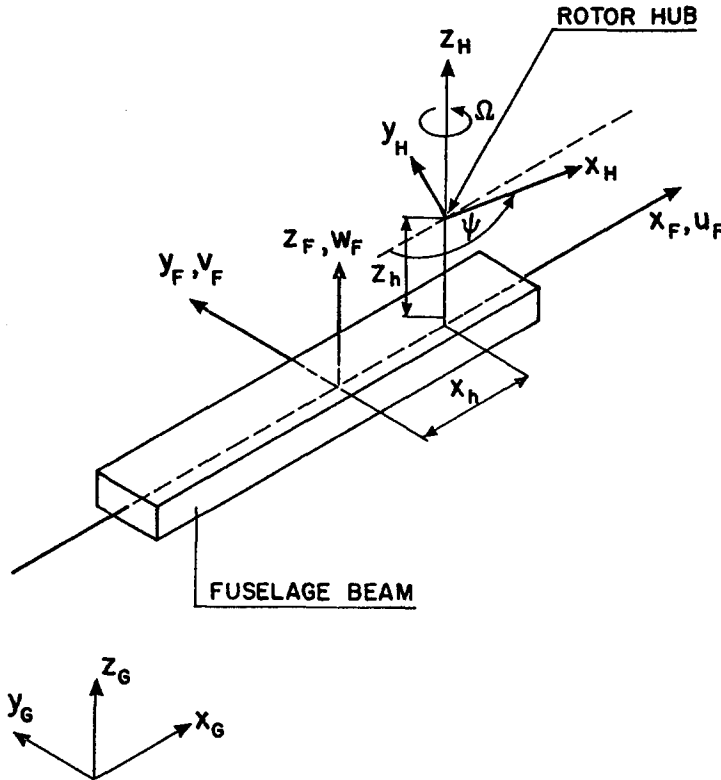


Figure 4. The “Gravity,” “Fuselage,” and “Hub” systems of coordinates.

The G (gravity) system is an inertial reference system while gravity is assumed to act in the $-\hat{z}_G$ direction.

The F (fuselage) system is a system which is attached to the fuselage (see Figure 4). The transformation between the G system and the F system is a function of the fuselage attitude angles θ_{Fx} , θ_{Fy} , and θ_{Fz} . By setting $\theta_{Fz} = 0$, the helicopter fuselage is assumed to be placed in a plane which is parallel to the $\hat{x}_G - \hat{z}_G$ plane.

The H (hub) system is attached to the F system at the coordinate $x_F = x_h$, $z_F = z_h$ (see Figure 4) and is rotating in a constant angular velocity $\Omega \hat{z}_F$. The transformation between the F and the H systems is a function of the azimuth angle of the reference blade, ψ .

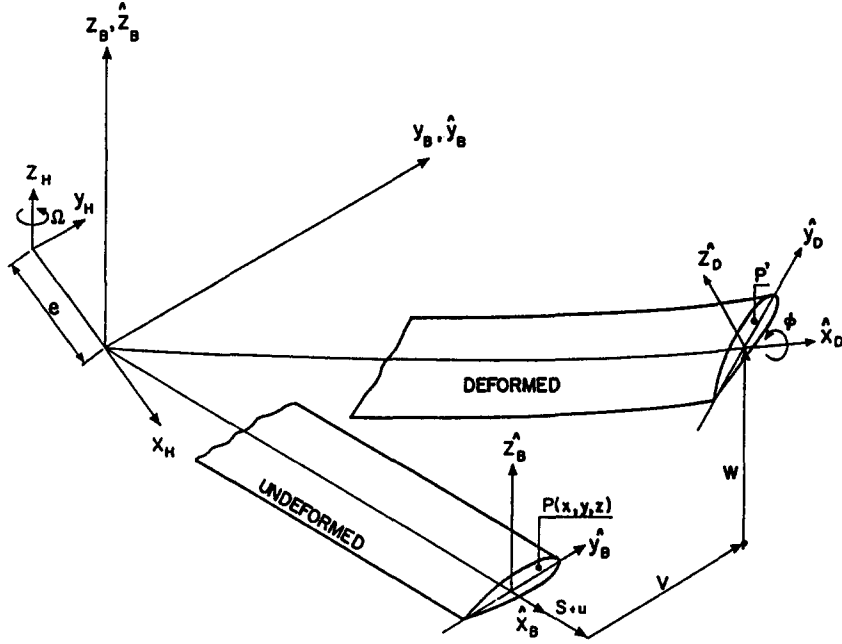


Figure 5. The "Hub," "Blade," and "Deformed" systems of coordinates.

The B (blade) system is connected to the H system at $e\hat{x}_H$ and its attitude is determined by the three root angles β, ζ, θ . β is the flapping angle, ζ is the lead-lag angle and θ is the pitch angle.

The D (deformed) system is a local system of coordinates which is attached to each cross-section along the blade (see Figure 5). The attitude of this system is determined by the local elastic displacements u, v, w in the $\hat{x}_B, \hat{y}_B, \hat{z}_B$ directions, respectively, and the twist angle, ϕ , which is superimposed (about the elastic axis) over the above deformation. Before deformation, the blade elastic axis is assumed to be straight and to coincide with the x_B axis. While the elastic elongation of the blade is usually small, the present analysis accounts also for the shortening of the distance of each cross-section to the rotating axis induced by the transverse displacements. Thus, the location of the D system root is at $x_B = x + s$, $y_B = v$, $z_B = w$, where

$$s(x) \cong -\frac{1}{2} \int_0^x (w_x^2 + v_x^2) dx'. \quad (7)$$

3.2. The Blade Structural Modeling

The structural analysis is based on the generic nonlinear beam model described in [15]. The nonlinear equations in this model are derived for small strains and moderate elastic rotations. The bending moment components in this case are given by

$$M_x = \left(GJ + \frac{PI_p}{A} \right) T, \quad (8a)$$

$$M_y = -EI_{yz}K_y - EI_{zz}K_z + Pz_c, \quad (8b)$$

$$M_z = EI_{yy}K_y + EI_{yz}K_z - Py_c. \quad (8c)$$

P is the tensile force (which has replaced u as an unknown), and y_c, z_c are the cross-sectional coordinates of the center of tension. K_y, K_z and T are the curvatures in \hat{y}_D and \hat{z}_D directions, and the twist, respectively. These curvatures are given by the following nonlinear expressions:

$$T = \phi_{,x} + (v_{,xx} + w_{,xx} \phi)(w_{,x} - v_{,x} \phi), \quad (9a)$$

$$K_y = v_{,xx} + w_{,xx} \phi, \quad (9b)$$

$$K_z = w_{,xx} - v_{,xx} (\phi + v_{,x} w_{,x}), \quad (9c)$$

where $(\)_{,x}$ stands for differentiation with respect to the blade length. The six equilibrium equations for forces and moments that act on each segment of the beam are also presented in [15]. Elimination of the shear resultant forces from these equations (by expressing them as functions of the above moments and curvatures) yields the following four differential equations of equilibrium:

$$P_{,x} = -p_x + K_y V_y + K_z V_z, \quad (10a)$$

$$K_y P - (EI_{yy} v_{,xx} + EI_{yz} w_{,xx}),_{xx} = -p_y + TV_z + q_{ze,x}, \quad (10b)$$

$$K_z P - (EI_{yz} v_{,xx} + EI_{zz} w_{,xx}),_{xx} = -p_z - TV_y - q_{ye,x}, \quad (10c)$$

$$\left[\left(GJ + \frac{PI_p}{A} \right) T \right]_{,x} = -q_x + K_y M_y + K_z M_z, \quad (10d)$$

where q_{ze}, q_{ye} are equivalent load components that contain the actual loads and additional nonlinear contributions. The nonlinear expressions for the equivalent loads and the associated boundary conditions are given in [15].

The equations of motion are obtained by substituting the inertia and aerodynamic loads which will be mentioned in what follows in the right hand side of equations (10a-d). These are differential equations in time and space. The unknowns in these equations are functions of the time and the beamwise coordinate along the blade. Using Galerkin's method, these equations are converted into differential time dependent equations for the shape function coefficients. These coefficients are then expressed as Harmonic Variables. Note that any other treatment of the problem in space could be utilized while the time domain is handled by the Harmonic Variable method as described in Section 2.

3.3. The Elastic Fuselage

The fuselage and its system of coordinates x_F, y_F and z_F are presented schematically in Figure 4. The formulation is based on modal analysis and it is assumed that the motion consists of small linear deflections in which all elastic lateral and twist motions are uncoupled (longitudinally, the fuselage is assumed to be infinitely stiff). Thus, the fuselage deformation may be expressed as

$$w_F(x_F, t) = \sum_{i=1}^{N_w} \xi_w^i(t) \cdot \Phi_w^i(x_F), \quad (11a)$$

$$v_F(x_F, t) = \sum_{i=1}^{N_v} \xi_v^i(t) \cdot \Phi_v^i(x_F), \quad (11b)$$

$$\phi_F(x_F, t) = \sum_{i=1}^{N_\phi} \xi_\phi^i(t) \cdot \Phi_\phi^i(x_F). \quad (11c)$$

As a beam, the fuselage boundary conditions are "free" at both ends. To account for rigid motions, the first modes have been chosen as follows:

$$\Phi_w^1 = \Phi_v^1 = \Phi_\phi^1 = 1; \quad \phi_w^2 = \Phi_v^2 = \frac{x_F - x_{FCG}}{L_F}, \quad (12)$$

where x_{FCG} and L_F are the fuselage center of gravity coordinate and its length, respectively, and the successive modes are the corresponding natural mode shapes.

Generally, in a trimmed forward flight, the helicopter fuselage undergoes periodic excitation due to many sources. Even by confining the discussion to the vibration induced by the main rotor, in certain configurations one should take into account not only the vibrations which are transferred to the fuselage through the hub, but also those vibrations which are induced by the blades passage over the fuselage, or by the interaction of the main rotor wake with the fuselage. However, the study presented in this paper is restricted to the vibratory forces and moments which are transferred to the fuselage through the hub. All other loads acting over the fuselage are assumed to contain relatively low frequencies.

Based on the above assumptions, the fuselage accelerations components at $x_F = x_P$ due to the p^{th} harmonic of the hub loads may be put in the following form:

$$\begin{bmatrix} \bar{G}_x & 0 & 0 & 0 & 0 & 0 \\ 0 & \bar{G}_y & 0 & 0 & 0 & \bar{R}_z \\ 0 & 0 & \bar{G}_z & 0 & \bar{R}_y & 0 \\ 0 & 0 & 0 & \bar{R}_x & 0 & 0 \end{bmatrix} \begin{Bmatrix} \bar{F}_x \\ \bar{F}_y \\ \bar{F}_z \\ \bar{Q}_x \\ \bar{Q}_y \\ \bar{Q}_z \end{Bmatrix} = \begin{Bmatrix} \bar{u}_F \\ \bar{v}_F \\ \bar{w}_F \\ \bar{\phi}_F \end{Bmatrix}, \quad (13)$$

where $(\bar{\cdot})$ indicates a complex quantity which consists of a magnitude and a phase angle. \bar{F}_α and \bar{Q}_α ($\alpha = x, y, z$) are the forces and moments at the hub ($x_F = x_h$), respectively, while \bar{G}_α and \bar{R}_α ($\alpha = x, y, z$) are their influence coefficients, respectively. These quantities are defined as

$$\bar{F}_\alpha = F_\alpha e^{i(p\psi - \phi_\alpha^F)}, \quad (14a)$$

$$\bar{Q}_\alpha = Q_\alpha e^{i(p\psi - \phi_\alpha^Q)}, \quad (14b)$$

$$\bar{G}_\alpha = G_\alpha e^{-i\beta_\alpha^F}, \quad (14c)$$

$$\bar{R}_\alpha = R_\alpha e^{-i\beta_\alpha^Q}. \quad (14d)$$

It should be noted that the values of F_α , Q_α , G_α , R_α , ϕ_α^F , ϕ_α^Q , β_α^F , β_α^Q are all functions of the harmonic number, p , the hub location, x_h , and the location where the acceleration response is obtained, x_p . The assumption of linear behavior of the fuselage allows one to sum up the accelerations due to each harmonic separately.

To demonstrate the analytic evaluation of the above influence coefficients, the following discussion will be concentrated on the vertical motion, w_F . Therefore, for the sake of clarification, the index $(\cdot)_w$ will be omitted in what follows. Since Φ^i are orthogonal modes, the governing equation for the i^{th} mode becomes:

$$M^i \xi^i \Omega^2 + M^i C^i \xi^i \Omega + M^i \omega^{i^2} \xi^i = F_z(\psi) \Phi^i(x_h) - Q_y(\psi) \frac{\partial \Phi^i}{\partial x_F}(x_h), \quad i = 1, N, \quad (15a)$$

where

$$M^i = \int_0^{L_F} \phi^{i^2}(x'_F) m(x'_F) dx'_F, \quad (15b)$$

C^i is a generalized damping coefficient, ω^i is the i^{th} mode frequency, m is the fuselage mass per unit length and $F_z(\psi) (= \text{Re}(\bar{F}_z))$ and $Q_y(\psi) (= \text{Re}(\bar{Q}_y))$ are the concentrated force and moment in the z_F and y_F directions, respectively, that act at the hub ($x_F = x_h$). $(\cdot)^*$ stands for differentiation with respect to the azimuth angle, ψ . As shown, the damping is assumed to be proportional to the mass per unit length in order to preserve the mode orthogonality. However, C^i may be a function of ω^i as experimentally observed in typical rotorcraft fuselages.

Solving equation (15a) for all ξ^i ($i = 1, N$) and based on the notation of equation (13), it may be shown that G_z and β_z^F are given by

$$G_z(p, x_h, x_p) = p^2 \Omega^2 \sqrt{\left[\sum_{i=1}^N \frac{A^i \Phi^i(x_h) \Phi^i(x_p)}{A^{i2} + B^{i2}} \right]^2 + \left[\sum_{i=1}^N \frac{B^i \Phi^i(x_h) \Phi^i(x_p)}{A^{i2} + B^{i2}} \right]^2}, \quad (16a)$$

$$\beta_z^F(p, x_h, x_p) = \arctg \left(\frac{\sum_{i=1}^N \frac{B^i \Phi^i(x_h) \Phi^i(x_p)}{A^{i2} + B^{i2}}}{\sum_{i=1}^N \frac{A^i \Phi^i(x_h) \Phi^i(x_p)}{A^{i2} + B^{i2}}} \right), \quad (16b)$$

where

$$A^i = M^i(\omega^{i2} - p^2 \Omega^2), \quad (17a)$$

$$B^i = M^i C^i p \Omega. \quad (17b)$$

Similar analytic expressions may be derived for G_x , G_y , R_x , R_y , R_z , β_x^F , β_y^F , β_x^Q , β_y^Q , β_z^Q , (see [14]).

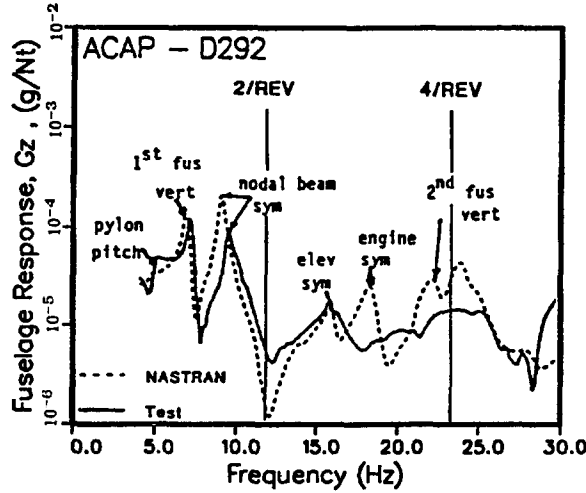


Figure 6a. Fuselage absolute response (G_z at the pilot seat) as a function of the frequency of the hub vibratory force as obtained in ground shake tests [16]).

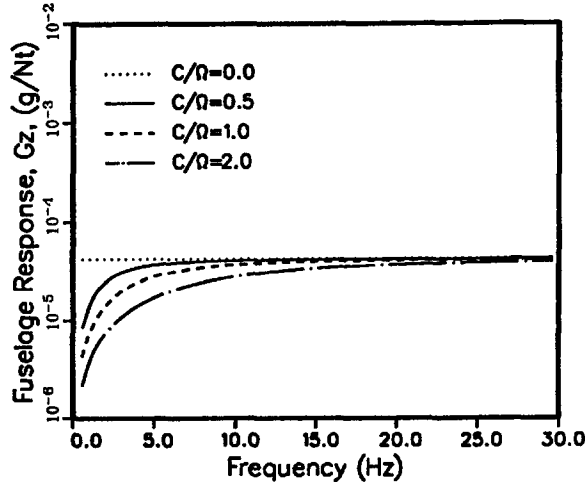


Figure 6b. Fuselage absolute response (G_z at the pilot seat) as a function of the frequency of the hub vibratory force as obtained by the analytic model using rigid modes only.

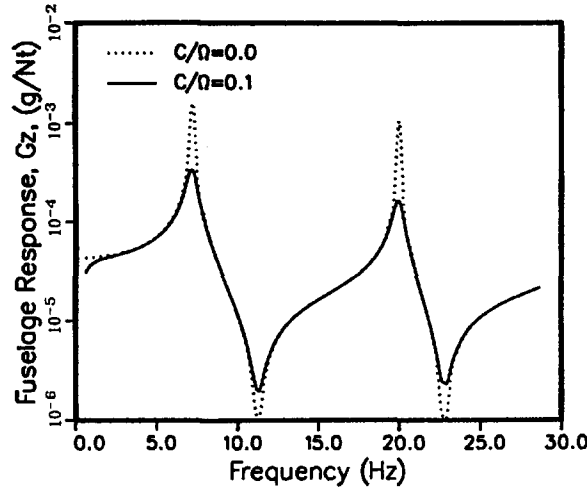


Figure 6c. Fuselage absolute response (G_z at the pilot seat) as a function of the frequency of the hub vibratory force as obtained by the analytic model using rigid and elastic modes of uniform beam.

Figures 6a–c present the quality of results that may be obtained by the above assumptions. Figure 6a (reproduced from [16] for the ACAP fuselage) presents typical variation of the value of G_z at the pilot seat location (x_p) as a function of the exciting frequencies p . Figures 6b–c show the analytic results that were obtained by assuming rigid body modes or by assuming uniform elastic beam model for different values of damping. As shown, assuming rigid fuselage is not acceptable, and there are many missing details in the elastic beam results as well.

Having clarified this point, there are three alternative ways to study the fuselage influence. The first one is to accept the above quality of results and to derive analytically the influence coefficient based on the mass and stiffness distribution of the fuselages (as presented above by equations (13), (16), (17)). A second way is to execute similar calculations using more refined structural/dynamic analysis of the fuselage as a three dimensional structure. A third alternative way has been adopted for the present study where a parametric study of the fuselage reaction as a function of the “global” responsiveness parameters \bar{G}_α , \bar{R}_α has been carried out. This alternative seems to be efficient due to the fact that many different fuselage structures may have the same hub reaction as reflected by \bar{G}_α , \bar{R}_α . In addition, the prediction of the damping mechanisms that control the phase of the fuselage reaction seems to be a complicated task and meanwhile may be extracted mainly from experimental data. For all the above alternatives, the fuselage influence may be introduced to the analysis by equations similar to equation (13) since the rotor is excited only by the fuselage motion at the hub, and the fuselage is excited only by the hub loads. Note that if the analysis is a nonlinear and a three dimensional one, the matrix in equation (13) may be fully populated and there may be couplings between the harmonics.

3.4. The Inertial Loads

To determine the inertial loads at a certain cross-section in the local D system, one has to express the inertial acceleration (i.e., in the G system) of each material point over the cross-section. This process has been carried out systematically and consistently by sequential usage of all the transformation matrices. However, since all the participating degrees of freedom were defined as Harmonic Variables, this process is simple and is reduced to the coding of the transformation operations and the required integrations. The end result is the inertial loads expressed as Harmonic Variables as well. More details may be found in [14].

3.5. The Aerodynamic Loads

To determine the aerodynamic loads, one first has to evaluate the components of the resultant “dynamic” velocity at each cross-section (i.e., the velocity due to the fuselage motion, the rotor

rotation, the elastic motions, etc.). Since the present analysis deals with motions containing high harmonics, exact and complete expression of the dynamic velocity which is fully consistent with the dynamic response is required. This step has been executed similar to the above inertial loads based on the exact transformation matrices. The end result of this step is the velocity components at each cross-section expressed as Harmonic Variables.

The expressions for the aerodynamic loads are based on a two-dimensional unsteady strip theory obtained from the classical Theodorsen theory and its extension to the case of pulsating free stream velocity provided by Greenberg (see [17]). These calculations account also for a prescribed steady inflow distribution over the disk. The assumption of steady inflow may be rationalized by the fact that the present modelling is concentrated on the case of a steady trimmed flight where the overall thrust and moments acting on the fuselage are constants. On the other hand, the local variations of loads are rapid, and unsteady evaluation of the loads which account for the near shed wake effects is inevitable. The end result of these calculations is the aerodynamic loads expressed as Harmonic Variables (see [14]).

3.6. Hub Loads

The hub loads are obtained by direct integration of the distributed loads over the blade. For that purpose, all distributed loads and moments originally developed in the D system are first transformed to be B system. Then, all quantities are integrated to yield the blade root loads. These loads are then transformed through the offset to the H system. Such loads due to all blades are then assembled to give the resultant forces and moments in the non-rotating system.

3.7. Trim

To assure a trimmed steady flight, the present formulation is supplemented by seven equations which enable the introduction of seven unknown trim parameters. These unknowns are the fuselage steady (mean) attitude angles θ_{Fx0} and θ_{Fy0} ($\theta_{Fz} = 0$ is assumed), the collective pitch angle (θ_0), the cyclic pitch angles (θ_{1C} and θ_{1S}), the tail rotor thrust, and the averaged induced velocity. The corresponding equations are based on equilibrium of forces and moments in the F system (six equations) and on Glauert's momentum equation for the averaged inflow. Note that

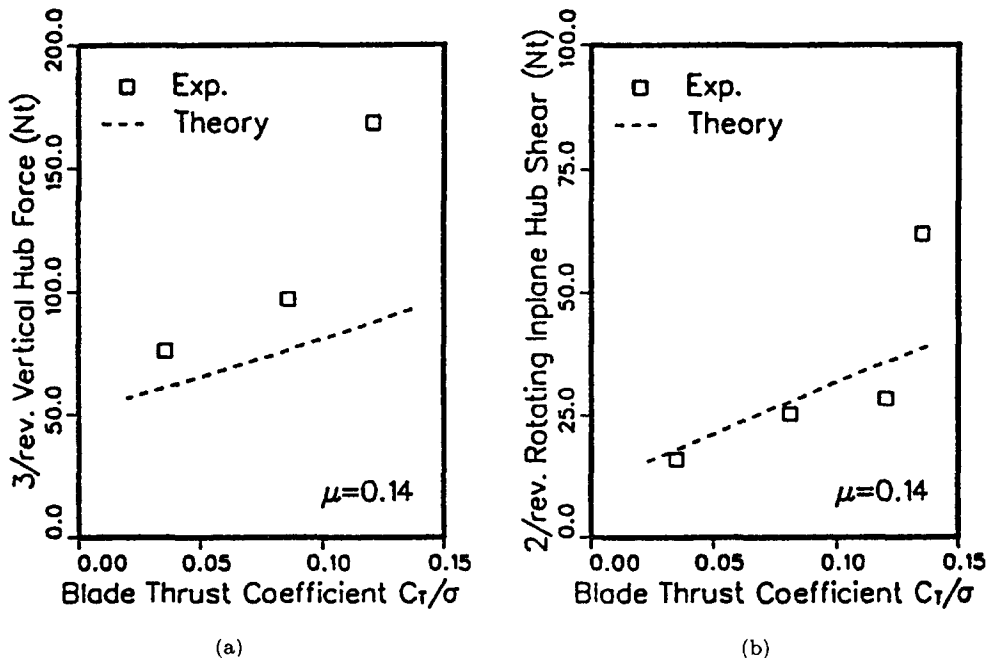


Figure 7. Correlation of the present results with wind tunnel measurements [18].

this is a fully coupled aeroelastic trim where all degrees of freedom simultaneously participate in the solution.

3.8. Illustrative Examples

To demonstrate the need for high harmonic resolution, correlations with test results reported in [18] are presented first. In this test, a three-bladed rotor was mounted in a wind tunnel (and therefore, the calculated results contain no fuselage influences), and the resulted vibratory hub loads at advance ratio of 0.14 were measured. The correlation is presented in Figure 7. To appreciate the quality of the results, one should realize that the nonrotating hub force (Figure 7a) is only 1.3% of the thrust and the rotating in-plane force (Figure 7b) is about 2% of the thrust.

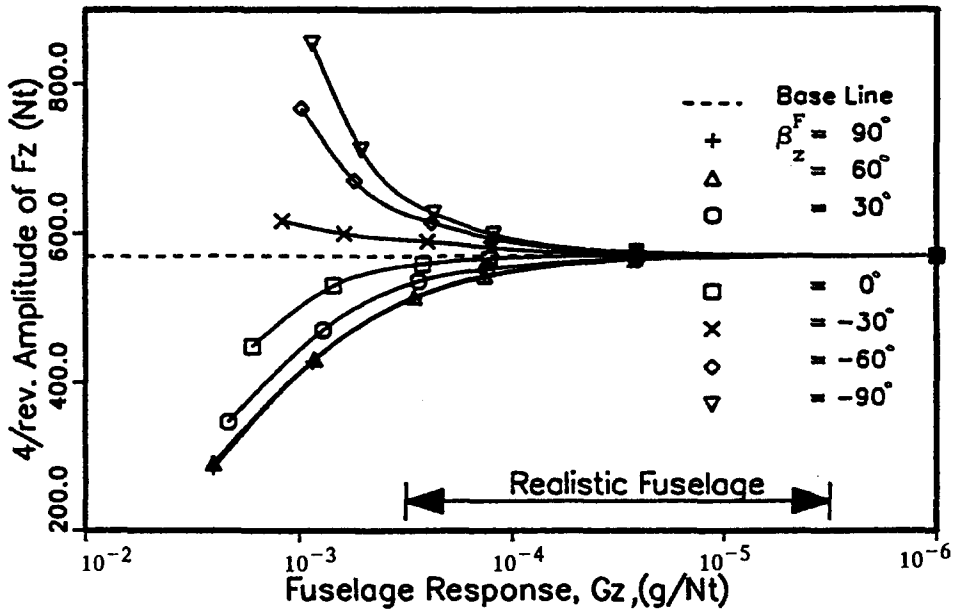


Figure 8a. The fuselage influence on F_z as function of its response magnitude, G_z , and phase, β_z^F .

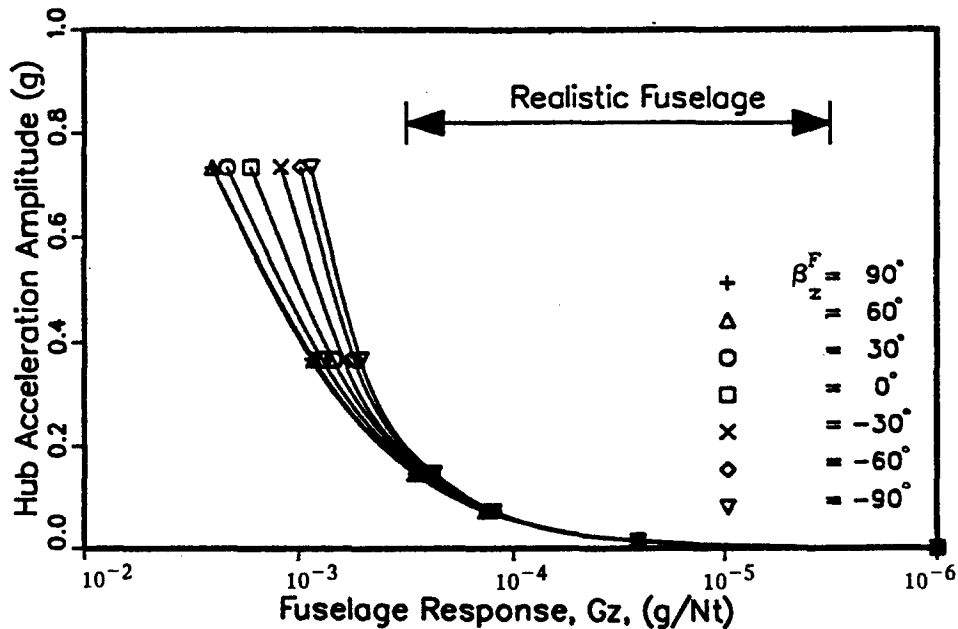


Figure 8b. The fuselage influence on hub acceleration as function of its response magnitude, G_z , phase, β_z^F .

A study of the influence of realistic elastic fuselage on the vibratory characteristics of rotor/fuselage systems is presented next. The following results are for a typical full-scale system in forward flight where the rotor consists of four hingeless blades ($\mu = 0.3$, $C_T = 0.009$). To demonstrate the use of the "global" responsiveness parameters as discussed in Section 3.3, the following examples deal with the most important component of the fuselage vibratory response—the vertical motion. Therefore, the only nonzero parameters are G_z , β_z^F , R_y , β_y^Q .

Figure 8a presents the 4/rev. amplitude of the vertical force, F_z , which is transferred to the fuselage as a function of G_z for different values of β_z^F ($R_y = 0$ in this case). The realistic range of the fuselage response is also indicated (see also Figure 6a). The corresponding values of the phase lag angle depend mainly on the overall damping of the fuselage structure, and therefore, a wide range of angles has been studied. Figure 8b presents the hub acceleration amplitude for each curve of Figure 8a. The symbols in Figures 8a,b represent constant acceleration. As shown, for very stiff and massive fuselage (i.e., for large values of G_z), the 4/rev. amplitude of F_z coincides with the case of an isolated rotor, while the hub acceleration amplitude vanishes. As the fuselage becomes elastic and less massive, the hub acceleration amplitude rises. As shown, it may be possible to adjust the fuselage structural damping (which reflects itself by the phase angle, β_z^F) so that for a given value of G_z , both hub acceleration amplitude and the vibratory force amplitude will be reduced. It should be emphasized that G_z and β_z^F are global parameters of the fuselage response and their values contain also the influence of isolation mechanisms or other vibration suppression devices that may be installed between the rotor and the fuselage. Such mechanisms are mostly efficient in modifying the value of β_z^F .

The influence of adding the fuselage response due to the vibratory hub moment in the y_F direction, Q_y , is presented in Figures 9a,b. As shown, the influence of this moment may be important. The general trends are similar to those observed in the case of vibratory vertical force. As the fuselage responsiveness to moment is reduced (i.e., large values of R_y) the vibration level coincides with those presented in Figure 8a. The hub acceleration amplitude as a function of R_y is presented in Figure 9b.

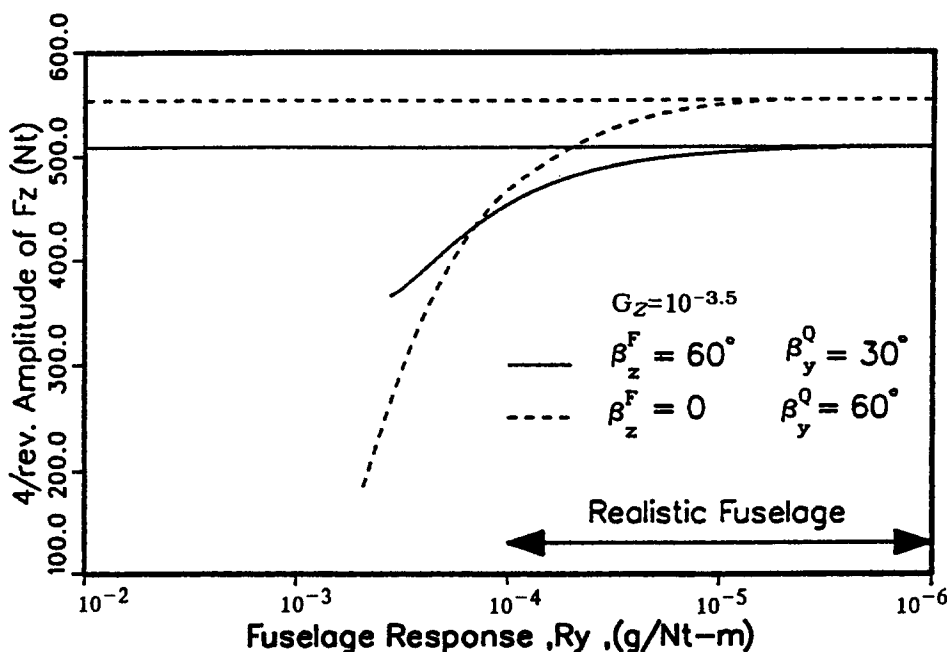


Figure 9a. The fuselage influence on F_z as a function of R_y for different phase angles, β_z^F , β_y^Q (for constant value of G_z).

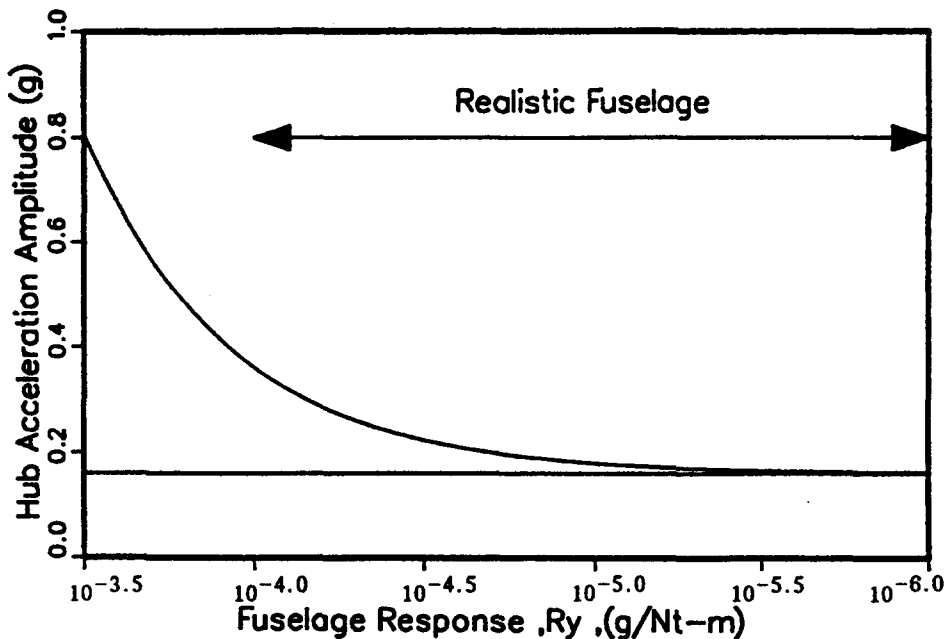


Figure 9b. The fuselage influence on the hub acceleration as a function of R_y for different phase angles, β_z^F , β_y^Q (for constant value of G_z).

The influence of elastic fuselage on the effectiveness of the higher harmonic pitch command is presented in Figure 10. In this case, the 4/rev. vibratory load is presented for various phase angles of the command with and without the fuselage. The fuselage is assumed to respond in the vertical direction only. Note that the θ_H pitch angle is superimposed on the trim pitch commands. Generally, it may be concluded that while the fuselage has influence on the hub loads, its influence on the higher harmonic control effectiveness and on the optimal phase angle is small.

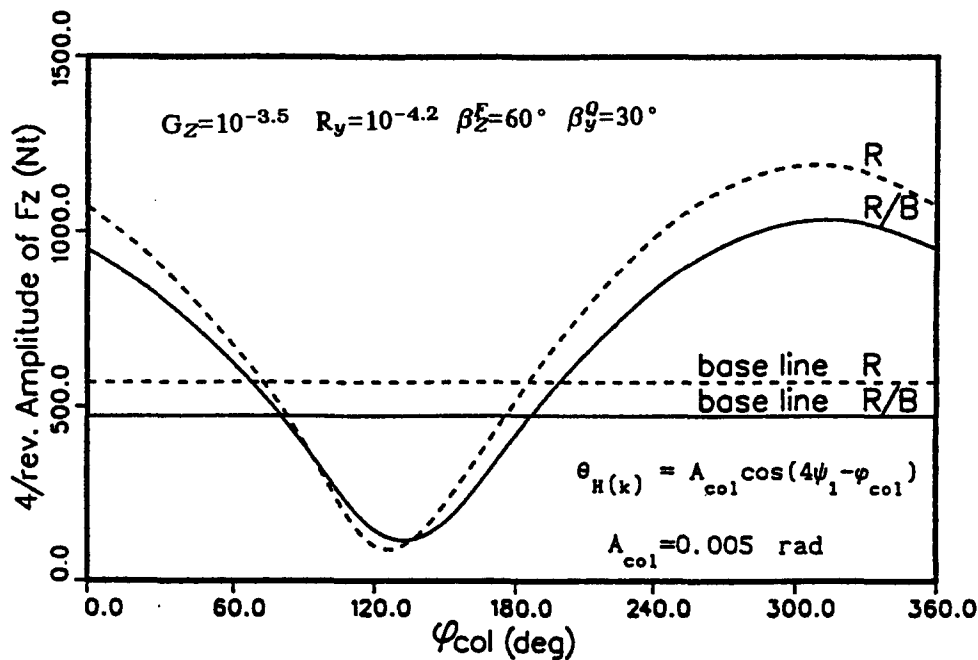


Figure 10. The influence of elastic fuselage on the effectiveness of the higher harmonic pitch command.

4. CONCLUDING REMARKS

A numerical technique for deriving and solving the nonlinear periodic equations of motion of a coupled rotor/fuselage system has been presented. The method substantially reduces the analytical and coding efforts which are required for implementation of the nonlinear periodic equations of motion, while preserving high accuracy solution and symbolic harmonic resolution. By using this method, the introduction of the equations of motion is confined to a simple listing of the equations while no time discretization or other adaptations are required. The present approach has been demonstrated by modelling a rotor/fuselage system that consists of elastic blades and fuselage and a study of the influence of the fuselage response characteristics.

REFERENCES

1. P.P. Friedmann, Helicopter rotor dynamics and aeroelasticity: Some key ideas and insights, *Vertica* **14** (1), 101–121 (1990).
2. R.E. Wood, R.W. Powers, J.H. Cline and C.E. Hammond, On developing and flight testing a higher harmonic control system, *J. Am. Helicopter Soc.* **30** (1), 3–20 (January 1985).
3. K. Nguyen and I. Chopra, Application of Higher Harmonic Control (HHC) to hingeless rotor systems, AIAA Paper No. 89–1215–CP, *Proc. AIAA/ASME/ASCE/ACS 30th Structures, Structural Dynamics and Materials Conf.*, Mobile, AL, April 1989, pp. 507–520.
4. I. Papavassiliou, P.P. Friedmann and C. Venkatesan, Coupled rotor/fuselage vibration reduction using multiple frequency blade pitch control, Paper No. 91–76, *Proceedings Seventeenth European Rotorcraft Forum*, Berlin, Germany, September 24–26, 1991, pp. 91.76.1–91.76.44.
5. I. Papavassiliou, P.P. Friedmann and C. Venkatesan, Coupled rotor/fuselage vibration reduction using open-blade pitch control, *Mathl. Comput. Modelling* **18** (3/4), 131–156 (1993).
6. N.D. Ham, Helicopter individual-blade-control research at MIT 1977–1985, *Vertica* **11**, 109–122 (1986).
7. S. Vellaichamy and I. Chopra, Effect of modeling techniques in the coupled rotor-body vibration analysis, AIAA Paper 93–1360–CP, *Proceedings 34th AIAA/ASME/ASCE/AHS/ASC Structures, Structural Dynamics and Materials Conference*, La Jolla, CA, April 19–22, 1993, pp. 563–575.
8. J.A. Molusis, The importance of nonlinearity of the higher harmonic control of helicopter vibration, *39th Annual Forum of the AHS*, St. Louis, MO, (May 1983).
9. R.A. Ormiston and D.A. Peters, Hingeless helicopter rotor response with nonuniform inflow and elastic blade bending, *Journal of Aircraft* **9** (10), 730–736 (October 1972).
10. D.A. Peters and R.A. Ormiston, Flapping response characteristics of hingeless rotor blades by a generalized harmonic balance method, NASA TN D-7856.
11. T.-K. Hsu and D.A. Peters, Coupled rotor/airframe vibration analysis by a combined harmonic-balance, impedance-matching method, *Proceedings of the 36th Annual National of the American Helicopter Society*, Washington, DC, May 1980; and *Journal of the American Helicopter Society* **27** (1) (January 1982).
12. M.-S. Huang and D.A. Peters, Coupled rotor-body vibrations with inplane degrees of freedom, *Proceedings of the American Helicopter Society's 2nd Decennial Specialists Meeting on Rotorcraft dynamics*, Ames Research Center, Moffett Field, CA, November 7–9, 1984.
13. O. Rand, Harmonic variables—A new approach to nonlinear periodic problems, *Computers Math. Applic.* **15** (11), 953–961 (1988).
14. S.M. Barkai, Investigation of the periodic nonlinear coupled response of helicopter elastic rotor and body to higher harmonic control, M.Sc. Thesis, Dept. of Aerospace Eng., Technion–I.I.T., (1993).
15. A. Rosen and O. Rand, Numerical model of the nonlinear behavior of curved rods, *Computers and Structures* **22** (5), 785–799 (1986).
16. R.V. Dompka, *et al.*, Plan, formulate, and discuss a NASTRAN finite-element model of the BELL-ACAP helicopter airframe, Summary Report 699-099-218, December 1986.
17. J.M. Greenberg, Airfoil in sinusoidal motion in pulsating stream, NACA TN-1329 (1947).
18. J. Shaw, N. Albion, E.J. Harker and R.S. Teal, Higher harmonic control: Wind tunnel demonstration of fully effective vibratory hub force suppression, *41st Annual Forum of the American Helicopter Society*, Fort Worth, TX, (1985).